Imaging of pleural disease

Maged Hassan [1], Abdelfattah A. Touman[2], Elżbieta M. Grabczak [3], Søren H. Skaarup [4], Katarzyna Faber[3], Kevin G. Blyth [5,6,7] and Svitlana Pochepnia[8]

[1]Chest Diseases Department, Alexandria University Faculty of Medicine, Alexandria, Egypt. [2]Pulmonary Medicine Department, King Abdullah Medical City, Makkah, Kingdom of Saudi Arabia. [3]Department of Internal Medicine, Pulmonary Diseases and Allergy, Medical University of Warsaw, Warsaw, Poland. [4]Department for Respiratory Diseases and Allergy, Aarhus University Hospital, Aarhus, Denmark. [5]School of Cancer Sciences, University of Glasgow, Glasgow, UK. [6]Cancer Research UK Scotland Centre, Beatson Institute, Glasgow, UK. [7]Glasgow Pleural Disease Unit, Queen Elizabeth University Hospital, Glasgow, UK. [8]Medical University of Vienna AKH, Vienna, Austria.

Corresponding author: Maged Hassan (magedhmf@gmail.com)

Shareable abstract (@ERSpublications)
Chest radiographs are often the first imaging tests to point to a pleural pathology. With the exception of pneumothorax, ultrasound and/or CT scans are usually required to further characterise the pleural pathology and guide management. https://bit.ly/3RdAcQy

Cite this article as: Hassan M, Touman AA, Grabczak EM, *et al*. Imaging of pleural disease. *Breathe* 2024; 20: 230172 [DOI: 10.1183/20734735.0172-2023].

Received: 9 Oct 2023
Accepted: 1 Dec 2023

Abstract

The pleural space is a "potential" anatomical space which is formed of two layers: visceral and parietal. It normally contains a trace of fluid (~10 mL in each hemithorax). Diseases of the pleura can manifest with thickening of the pleural membranes or by abnormal accumulation of air or liquid. Chest radiographs are often the first imaging tests to point to a pleural pathology. With the exception of pneumothorax, and due to the inherent limitations of chest radiographs, ultrasound and/or computed tomography are usually required to further characterise the pleural pathology and guide management. This review summarises the utility of different imaging tools in the management of pleural disease and discusses new and evolving tools in imaging of the pleura.

General considerations

The pleural space is a "potential" anatomical space which is formed of two layers: visceral and parietal. It normally contains a trace of fluid (~10 mL in each hemithorax) [1]. The two pleural layers together have minute thickness and, in absence of pathology, are seen on computed tomography (CT) as a 1–2 mm "intercostal stripe" which comprises the pleural membranes as well as extra-pleural adipose tissue [2]. Diseases of the pleura can manifest with thickening of the pleural membranes or by abnormal accumulation of air or liquid.

Imaging of pleural abnormalities

Chest radiographs are often the first imaging tests to point to a pleural pathology. With the exception of pneumothorax, and due to the inherent limitations of chest radiographs, ultrasound (US) and/or CT scanning are usually required to further characterise the pleural pathology and guide management.

Pleural thickening occurs due to various inflammatory and infectious causes and is also a feature of pleural malignancy. A chest radiograph may demonstrate pleural thickening as a peripheral radio-opaque stripe or as an "apical" cap, but more subtle thickening is only visible on CT scans. A late (venous)-phase contrast-enhanced CT scan is the optimal imaging protocol to visualise pleural thickening [2]. On chest radiographs, basal thickening causes obliteration of the costophrenic angle (figure 1), simulating a small pleural effusion. These two abnormalities can be differentiated using CT or US. A distinct type of pleural thickening are "pleural plaques", which are localised areas of thickening with shelf-like edges that exhibit a geographical appearance on chest radiographs and commonly show calcification (figure 1) [3]. These distinct abnormalities are benign and are seen in people who have been exposed to asbestos [3].

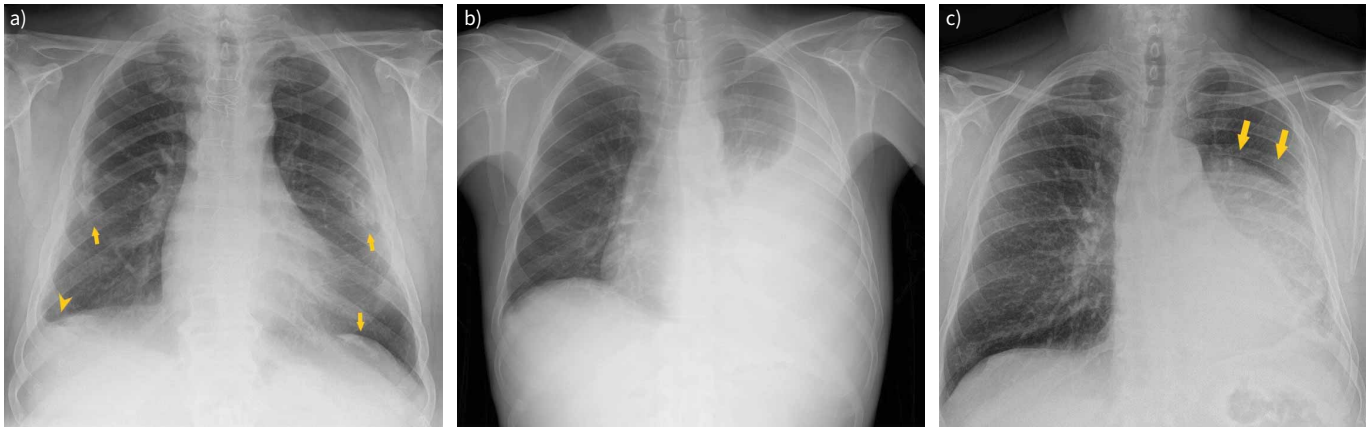

FIGURE 1 Chest radiographs (posterior–anterior projection) showing pleural thickening, plaques and effusion. a) Bilateral upper zone and diaphragmatic pleural plaques (arrows) and right basal pleural thickening (arrowhead). b) Large free-flowing pleural effusion in the left side. c) Rounded haziness (arrows) caused by left encysted pleural effusion.

As little as 175 mL of pleural fluid can blunt the costophrenic angle on a posteroanterior chest radiograph, but a smaller effusion can be detected on a lateral view [4]. It has been shown that chest radiographs miss more than 10% of a size-significant effusion that warrants thoracentesis especially in cases of lower lobe consolidation [5]. Free-flowing pleural effusions exhibit an upper-border, or "meniscus", on chest radiography whereby the homogeneous opacity has an upward concavity (figure 1). Encysted pleural effusions will have more abrupt edges (see the section on pleural infection) and may appear as haziness rather than dense opacification (figure 1).

Both CT and US have superior sensitivity in detecting pleural effusion in comparison to chest radiography and are able to reveal only few millilitres of fluid [6]. While US is more sensitive in demonstrating pleural fluid septations, mediastinal pockets of pleural fluid can only be visualised on CT [6].

This review summarises the utility of different imaging tools in the management of pleural disease including infection, malignancy and pneumothorax. Non-expandable lung and diaphragm disorders are also discussed. The review concludes with some data on new and evolving tools in imaging of the pleura.

Malignant pleural effusion

Malignant pleural effusion (MPE) is a common condition that develops in 15% of patients with metastatic cancer [7]. It is more commonly associated with secondary cancers (*i.e.* non-mesotheliomas), with lung cancer and breast cancer the most common primaries causing MPE in men and women, respectively [8]. In countries with a historical burden of asbestos use, such as the UK and Australia [8, 9], mesothelioma appears to be a common cause for MPE.

Malignant involvement of the pleura manifests with thickening and/or effusion. On CT scanning, smooth pleural thickening is usually a feature of benign disease, although thickening >1 cm is more suggestive of malignancy (figure 2) [10]. Nodularity of the pleura is virtually diagnostic of malignancy (figure 2). Leung *et al.* [10] found that circumferential thickening of the pleura, pleural nodularity, >1 cm thickness of parietal pleura, and involvement of mediastinal pleura had specificities of 100%, 94%, 94%, and 88%, respectively, for pleural malignancy. While being highly specific, these abnormalities are not universally present in malignant pleural disease. In a study including 211 patients with biopsy confirmed MPE, pre-thoracoscopy CT scanning had a sensitivity of only 68% [11]. It is also notable that none of the malignant features cited above can reliably differentiate primary from secondary pleural malignancy.

Thoracic US can be used to identify MPE in patients presenting with a new pleural effusion. In a study carried out in the radiology department, the presence of parietal or diaphragmatic pleural nodularity, pleural thickening >1 cm, or liver deposits on thoracic US were used to diagnose MPE [12]. Thoracic US had a sensitivity of 73% and specificity of 100% [12]. While such a diagnostic accuracy is impressive, it is important to remember that US is operator-dependent, and thus the experience of the operator will be a strong determinant in the correct elicitation and interpretation of US findings.

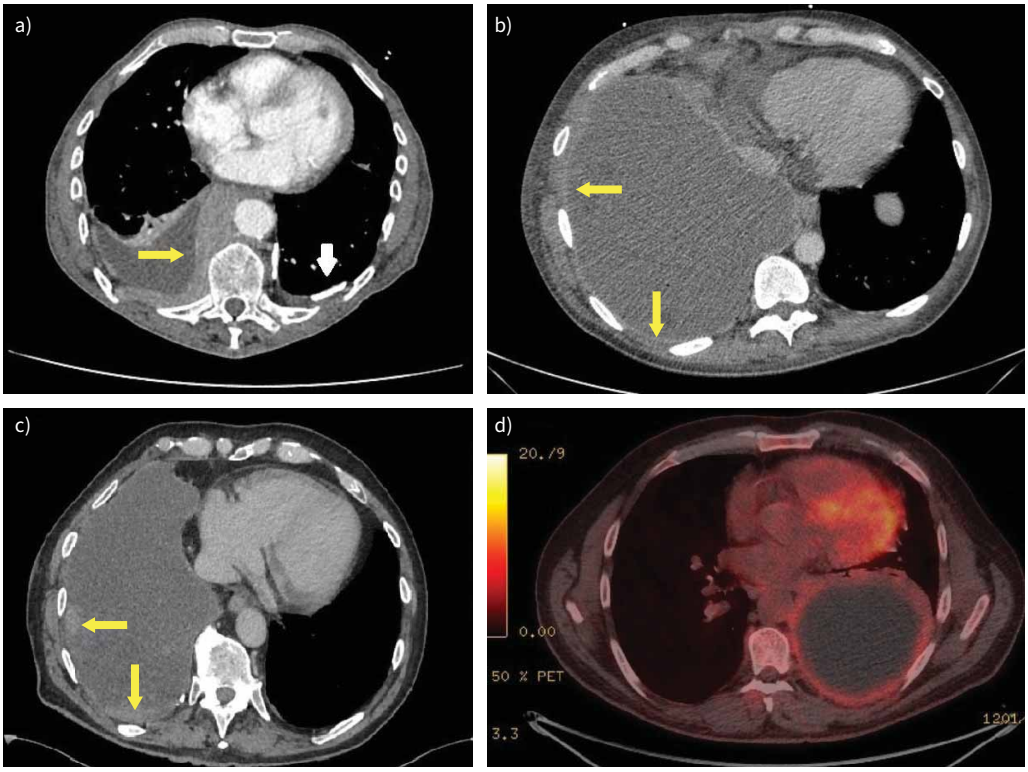

FIGURE 2 a–c) Contrast-enhanced computed tomography (CT) sections in mediastinal window showing different forms of parietal pleural thickening. a) Smooth enhancing pleural thickening >1 cm (yellow arrow) in a case of mesothelioma. Note the calcified pleural plaques (white arrow). b) Smooth pleural thickening in a case of empyema. c) Nodular pleural thickening in a case of metastatic lung cancer. d) Positron emission tomography-CT of a patient with left side empyema. Note radioactive tracer uptake of the thickened pleura.

Positron emission tomography (PET) scanning is not routinely requested in the diagnosis of MPE. However, PET scans may be helpful in MPE for identifying the primary malignancy in cases where other imaging modalities have not been helpful [13]. As with other cancers, pleural avidity on PET-CT is not pathognomonic of malignancy and can be seen in pleural infection (figure 2). In addition, pleural avidity on PET-scanning is seen after pleurodesis (due to pleural inflammation) and such avidity can persist for years. This is relevant where PET-CT is requested to rule out recurrence of pleural malignancy in patients who have previously been treated with pleurodesis [14].

Mesothelioma

Malignant pleural mesothelioma (MPM) is an uncommon asbestos-driven malignancy with a median survival of ∼18 months. 85% of patients present with a symptomatic pleural effusion, placing pleural imaging at the centre of the diagnostic pathway. Radiological quantification is also critical for staging and assessment of response to therapy, including combination immunotherapy, which significantly extends survival in some patients [15].

Imaging modalities

A chest radiograph is usually the first imaging test performed in suspected MPM. A unilateral, and often large, effusion may be the only visible abnormality, and emergence of a new effusion on a background of established pleural plaques is highly suspicious. Nodular pleural thickening, unilateral volume loss and fissural pleural thickening are all classically associated with MPM [16]; however, these are late radiographic features. Pleural plaques are consistent with asbestos exposure, but are commonly observed in patients who will never develop MPM [3].

CT remains the workhorse of the MPM pathway. In addition to effusion, CT will often reveal nodular, enhancing pleural thickening. Mediastinal, circumferential and fissural pleural thickening are typical of MPM [16, 17], but no CT parameter reliably differentiates MPM from secondary pleural cancers. CT is

significantly limited by poor tissue contrast between MPM and adjacent soft tissues/loculated fluid, translating into poor sensitivity (58–68%) in large series [11, 18]. This mandates a low threshold for invasive sampling if clinical suspicion is high. CT sensitivity is particularly low (27%) using CT pulmonary angiography and venous phase acquisition (69–90 s) is essential [18]. Peak contrast enhancement in a MPM tumour does not occur until 4.5 min on CT [19] and magnetic resonance imaging (MRI) [20], prompting delayed acquisition in some centres.

US is a key imaging modality in MPM, since most patients present with pleural effusion. US is cheap, highly portable and is associated with a reduced rate of visceral injury and improved sample yield during pleural fluid aspiration [21, 22]. US can also direct image-guided pleural biopsy. Sonographic features of MPM, including nodular pleural thickening >1 cm and diaphragmatic nodules, are highly specific (95–100%) but lack sensitivity (40%) [23], mandating further investigation if MPM is suspected clinically (similar to CT).

MRI does not yet have a routine role in the diagnostic MPM pathway but has distinct advantages over CT in early detection (figure 3). In early stage MPM, macroscopic pleural thickening may be absent, placing a premium on functional imaging tuned to other events, including neovascularisation. In a recent study of 58 patients, of whom 84% had a median pleural thickness <10 mm, perfusion MRI was associated with 92% sensitivity, compared with 56% sensitivity using CT [20]. Clinical deployment of MRI is currently limited by scanner availability and the increased scanning and reporting time required.

Disease staging, quantification and response assessment

MPM staging is primarily based on contrast-enhanced CT, with PET-CT and MRI reserved for specific questions in patients being considered for radical surgery. MRI has higher sensitivity than CT for chest wall and diaphragmatic invasion [24], which would both preclude radical resection. PET-CT has enhanced sensitivity to nodal and distant metastases [25], with 29% of patients having CT-occult extra-pleural disease in one previous study [26]. The recent negative results of the MARS2 trial of extended pleurectomy/decortication may reduce enthusiasm for such approaches in the future [27].

The complex morphology of MPM violates mathematical assumptions regarding spherical growth that underpin relationships between unidimensional tumour measurements and volume required for response assessment. Therefore, radiologists currently rely on a modified version of the RECIST (Response Evaluation Criteria In Solid Tumours) criteria for a best estimate of tumour response. However, these

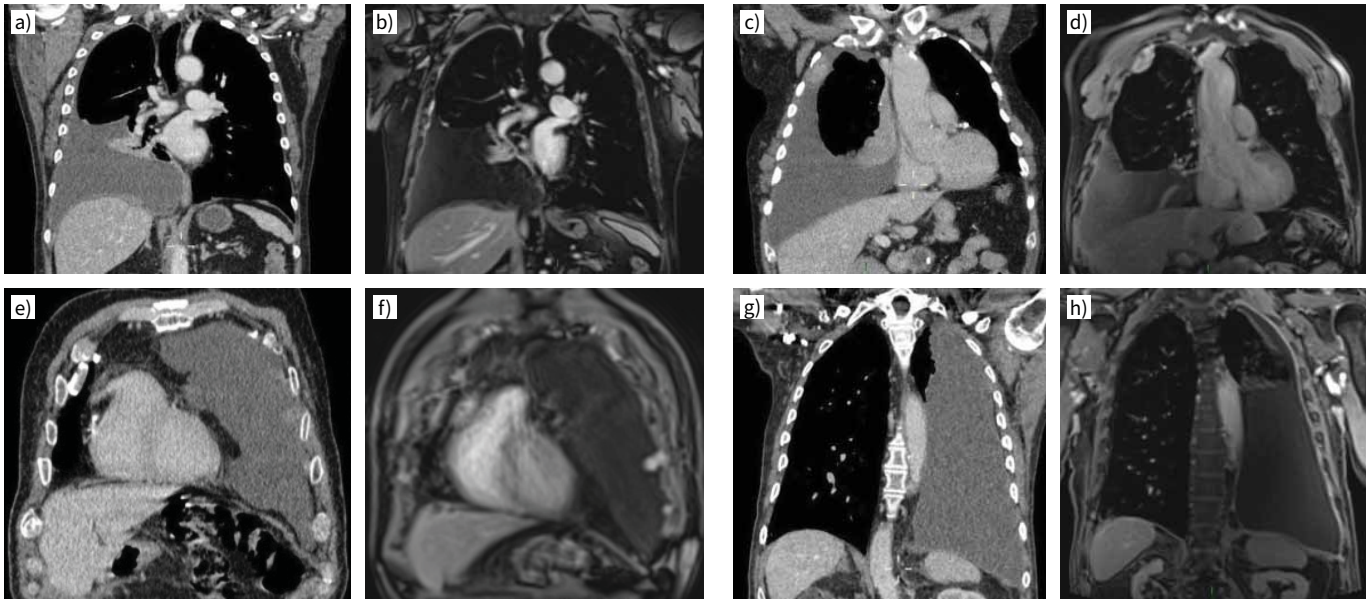

FIGURE 3 Contrast-enhanced magnetic resonance imaging (MRI) (b, d, f and h) and corresponding contrast-enhanced computed tomography (CT) images (a, c, e and g) in patients with malignant pleural mesothelioma. Panels a, b) and g, h) demonstrate low volume disease with minimal pleural thickening, while c, d) and e, f) demonstrate pleural-based mass lesions. In both settings, MRI offers superior soft tissue contrast over CT. Images courtesy of the authors of [20].

methods (currently version 1.1) are associated with high interobserver disagreement and up to 30% variance in total tumour measurements [28]. Direct measurement of MPM is the obvious alternative and although human measurements are prognostically valuable [29, 30] they are extremely laborious and inconsistent when applied by human readers [31]. This has prompted training and successful validation of a fully automated deep-learning artificial intelligence algorithm for CT volumetry [32], which should make MPM volume a more practical metric for future response assessment.

Pleural infection

The global burden and the incidence of pleural infection has been shown to have increased steadily over the past decade [33]. There is a significant overlap between the imaging features of infectious and non-infectious pleural diseases and in many cases diagnostic thoracentesis is required to ascertain the diagnosis. In this section we highlight the characteristic features of different imaging modalities focusing on bacterial and mycobacterial infection only.

Non-tuberculosis bacterial pleural infection

Infected pleural effusion can evolve into three stages which represent a continuous spectrum; however, each stage has its unique radiological and biochemical features [34]. These stages are: uncomplicated simple exudate (stage I), complicated fibrinopurulent (stage II) and organised empyema (stage III). Chest radiography and thoracic US are considered essential imaging modalities for diagnosis and drainage guidance of pleural infection [23].

Uncomplicated infected effusion on a chest radiograph is usually a unilateral, small, free-flowing effusion with an associated area of consolidation [23]. Primary pleural infection may occur in the absence of parenchymal lung infection, as a result of haematogenous spread or translocation of bacteria from an adjacent organ such as intra-abdominal infection [35]. When pleural infection progresses to fibrinopurulent and organised stages, it appears as a loculated pleural collection (figure 4a). Another feature which indicates a complicated pleural effusion is the presence of gas in the pleural space. Unless it resulted from an iatrogenic introduction of air into the pleural cavity during thoracentesis, it is termed pyopneumothorax and the gas source is a bronchopleural fistula or a gas-forming bacteria (figure 4) [7].

In stages II and III the infected effusion usually appears as turbid, loculated, septated or homogeneously echogenic fluid on US (figure 4b, c). The presence of small hyperechoic dots represents gas bubbles and

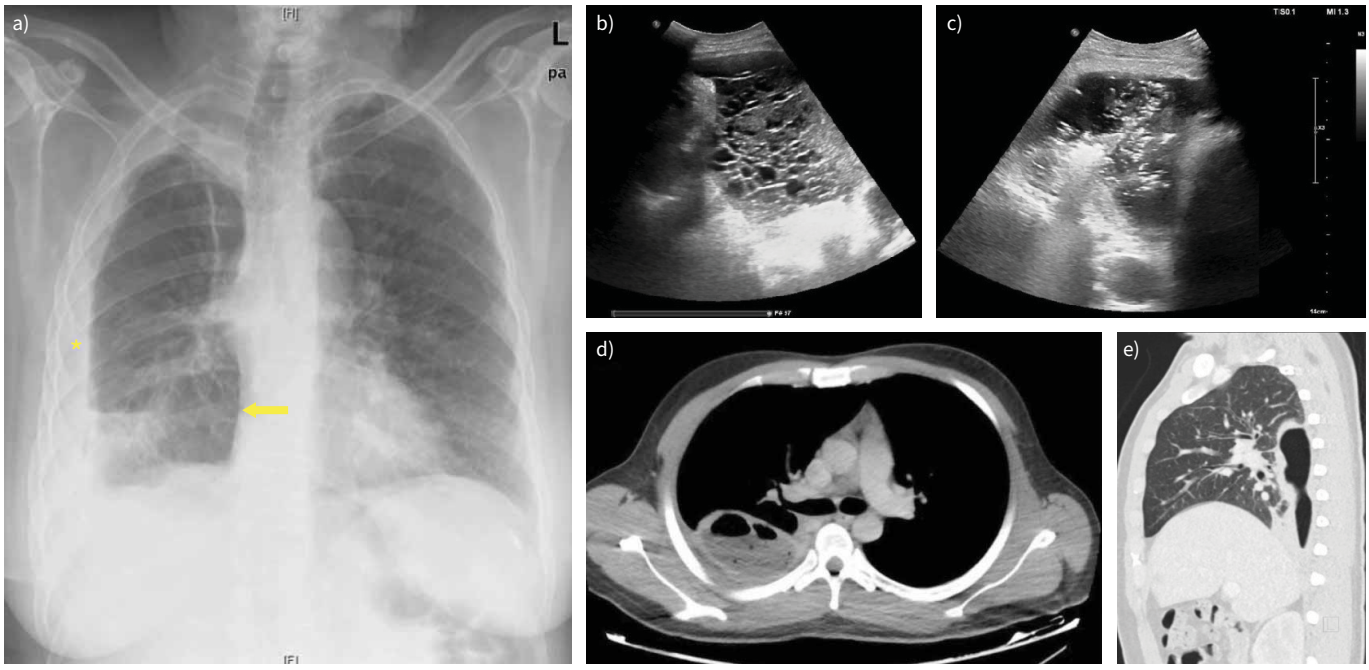

FIGURE 4 Imaging features of pleural infection on different modalities. a) Chest radiograph shows a laterally loculated pleural effusion on the right side (note the near-vertical free border of effusion). b, c) Thoracic ultrasound stills show septated pleural fluid and echogenic densities suggestive of pus. d, e) Computed tomography sections showing posteriorly loculated pyopneumothorax.

may indicate pyopneumothorax. However, the presence of anechoic effusion cannot differentiate between uncomplicated and complicated pleural effusion [36].

Chest CT scan is a frequently used modality to evaluate pleural infection. However, and similar to other imaging modalities, there are no pathognomonic features to differentiate infectious from non-infectious pleural disease [23]. On CT, oblong configuration, split pleural sign, hypertrophy and increased density of the extra-pleural fat, as well as the presence of ipsilateral consolidation, increase the likelihood of infectious aetiology [37]. It is sometimes difficult to differentiate lung abscess from empyema, but such delineation is important as it has a therapeutic implication (figure 4) [38]. Chest CT scan may also show moderately enlarged (<2 cm) mediastinal lymphadenopathy which is commonly associated with parapneumonic effusion. Larger mediastinal lymphadenopathy should rise suspicion of an alternative pathological process [39].

PET scans and MRI can image the pleura; however, they have a limited role in the management of parapneumonic effusions. On MRI imaging, parapneumonic effusions have a low signal on T1-weighted and high signal on T2-weighted. It is superior to CT in detecting pleural fluid septation and extra-pleural fat changes [40]. This imaging modality may be used in MPE to evaluate soft tissue invasion such as chest wall, diaphragmatic and spinal invasion [23].

Mycobacterial pleural infection

Tuberculous pleural effusions may result from primary infection or secondary (reactivation) disease [41]. Host immune status significantly increases the incidence of extrapulmonary tuberculosis including pleural tuberculosis (PTB), which is estimated to affect 6% in non-AIDS patients compared with 11% of AIDS patients [42].

On a chest radiograph, immune competent hosts commonly have unilateral, small to moderate effusion [41]. It is reported to be more common on the right side and is associated with parenchymal infiltrate in half of the cases [43]. By contrast, HIV-positive patients, regardless of CD4 count, are more likely to have bilateral pleural effusion and parenchymal infiltration than HIV-negative patients with odds ratios of 3.81 and 4.38, respectively [44].

Thoracic US allows characterisation of tuberculous fluid, which ranges from anechoic to septated, echogenic fluid [45]. The appearance of a complex, septated pleural fluid, which is found to be lymphocytic and exudative on analysis, has a positive predictive value of 94% for PTB [46]. However, none of the pleural sonographic features is pathognomonic for PTB. A concomitant pericardiac effusion may be detected in up to 6% of PTB cases [47]. In a multicentre Italian study, the presence of an enlarged (short axis >5 mm) internal mammary lymph node increased the likelihood of PTB, especially in patients <50 years of age with a positive predictive value of 87.8% [48]. In another pilot study, tuberculous pleurisy was found to be associated with apical consolidations (odds ratio 9.67) and subpleural nodules (odds ratio 5.30) [49]. Late sequelae of tuberculous pleurisy include localised pleural thickening and/or calcifications [50].

Thoracic US can be used as an image-guiding modality to biopsy thickened pleura [45]. Dissection of pus through the parietal pleura to the soft tissues of the chest wall is termed empyema necessitans and is a rare condition commonly caused by tuberculous mycobacterial infection and can be easily visualised on US (figure 5) [51].

Chest CT has the advantage of better visualising the lung parenchyma, thoracic lymph nodes and soft tissue. Involvement of these structures may have specific radiological features which are beyond the scope of this review. Focal smooth pleural thickening is reported to be the most common CT finding in PTB, it was reported to affect more than half of cases [52]. However, the circumferential, nodular thickness that exceeds 1 cm and involves mediastinal pleura which is highly suggestive of pleural malignancy has been reported to be seen in PTB as well [52]. Fibrothorax is a rare complication of PTB which is characterised by uniformly thickened pleura, with adhesion of the parietal and visceral pleura and loss of volume of the affected hemithorax [53]. Chest CT can add valuable clinical information by detecting other complications of PTB such as bronchopleural fistula or empyema necessitans [53]. Another rare complication of long-standing tuberculous empyema is pseudo-chylothorax, where a pathognomonic CT feature of fat-fluid or fat-calcium level is described in literature [54].

Pneumothorax

Pneumothorax appears when air enters the pleural cavity through either injury of visceral pleura and/or injury of the chest wall. It can be spontaneous (without an external factor) or traumatic/iatrogenic, affecting

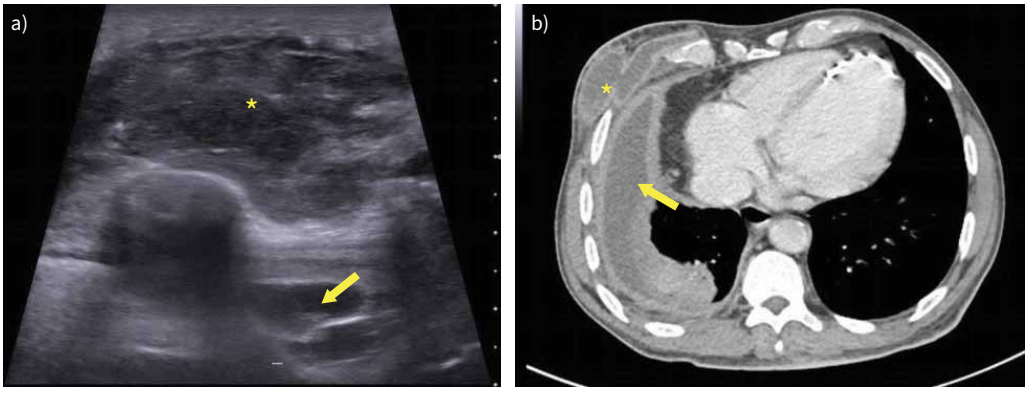

FIGURE 5 Tuberculous empyema complicated with empyema necessitans. a) Ultrasound and b) contrast-enhanced computed tomography show large intra-muscular collection (*); arrows indicate the tuberculous empyema.

either normal (primary spontaneous pneumothorax) or diseased lung (secondary pneumothorax). Air accumulating in the pleural cavity causes an increase in pleural pressure and partial or total ipsilateral lung collapse.

Chest radiography is the most frequently used imaging modality for diagnosis and management of spontaneous pneumothorax, while traumatic or iatrogenic pneumothorax is more frequently detected by chest US or CT first. The sensitivity of a chest radiograph is ~46% (95% CI 36–56.0), and depends on the patient's position; it can be as low as 20% in the supine position [55, 56]. Chest radiography has a specificity of 100% (95% CI 99–100%) [57].

In the upright position, air starts to collect in the apical region (the least gravitationally dependent part), more laterally than medially, pushing the lung away from the chest wall, which is visible as an opaque line of visceral pleura with aerated lung on the hilar side and more lucent (darker) pleural space filled with air on the chest wall side (figure 6). There is no need to perform expiratory radiographs as they do not show higher sensitivity in the diagnosis of pneumothorax [58, 59].

Depending on the size of pneumothorax, the lung may be completely compressed, and in cases of tension pneumothorax the mediastinum may be shifted to the contralateral side. Sometimes air may accumulate in other areas of the chest cavity as presented in figure 7. A sign that indirectly suggests the presence of air in the pleural cavity is a straight fluid horizontal line (figure 7), appearing when there is fluid and air in pleural space (hydropneumothorax).

In the case of a supine patient, air is most visible at the lung bases, increasing the lucency over the upper abdomen. Therefore, pneumothorax should be suspected when there is a sharp demarcation of the cardiac and mediastinal interfaces in anteromedial recess or there is a deep sulcus sign, double diaphragm sign or when subcutaneous gas is present in nonpenetrating trauma patients (figure 7) [60, 61]. Chest radiography in lateral decubitus position may show a small pneumothorax (15 mL of air) [62]. One should not forget about situations that may mimic pneumothorax (for details see table 1). Different formulas allow quantification of pneumothorax size and the making of therapeutic decisions (figure 6) [58, 63, 64].

A chest radiograph (with a lateral view) performed 1–4 h after drain insertion allows documentation of the resolution of pneumothorax, drain position, or possible complications.

US has become more popular in diagnostics of lung diseases, including pneumothorax. US detects pneumothorax with a sensitivity of 82.9% (95% CI 78.3–86.9%) and a specificity of 98.2% (95% CI 97.0–99.0%) and is better in neonates and trauma settings [55, 57]. The patient is examined in the supine position, as air moves to the front part of the chest in this position. The US probe (a linear one) is put parallel to the intercostal spaces between the II–IV rib (the least gravitationally dependent areas) close to the sternum and then moved laterally. Features of pneumothorax include abolished lung sliding, absence of lung pulse or comet-tail artefacts, and the presence of a lung point. In M-mode, it is typical to observe the stratosphere/barcode sign (supplementary videos). Unfortunately, US does not allow exact assessment of

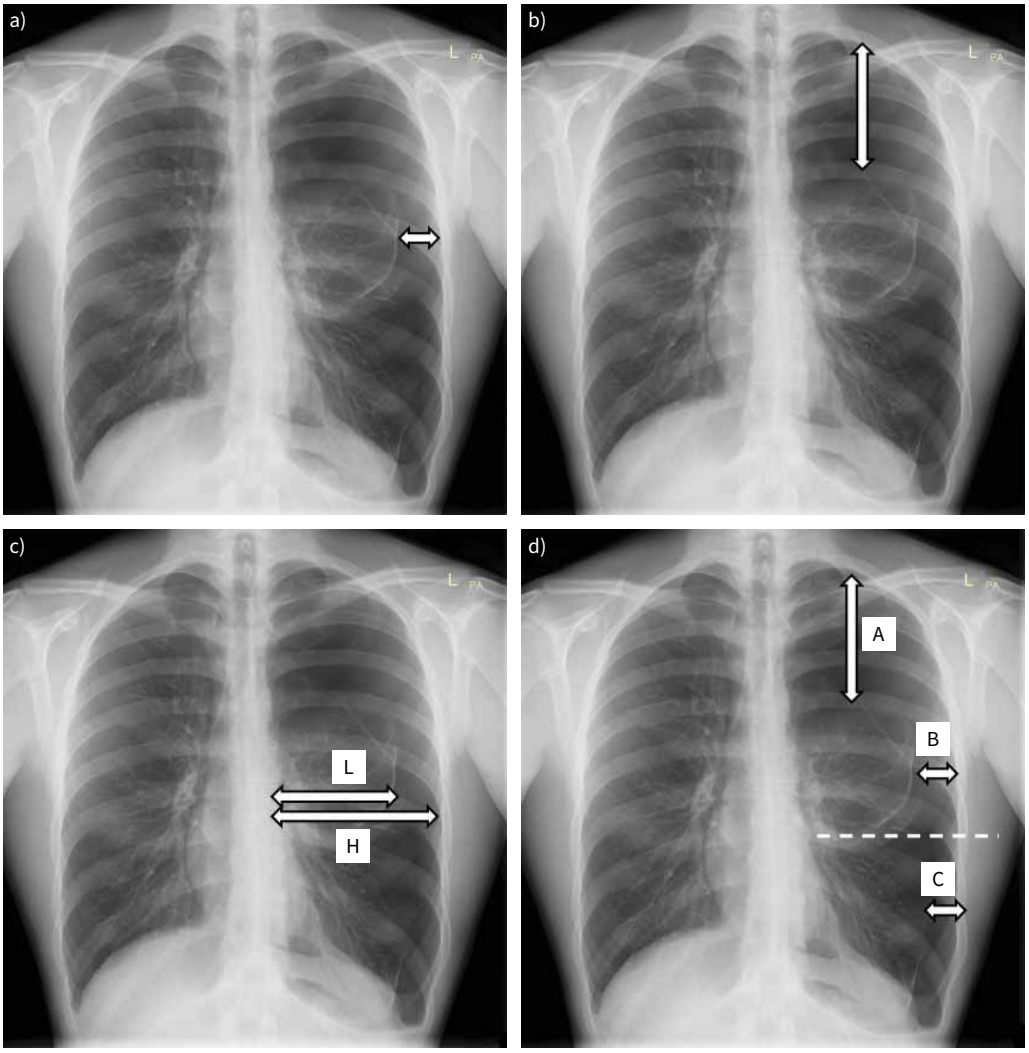

FIGURE 6 Different methods of measuring pneumothorax size on chest radiographs. a) Size is assessed based on the distance between the visceral pleura and chest wall on the level of the hilum; if ⩾2 cm big pneumothorax is diagnosed. b) Size is measured in the apex; if ⩾3 cm big pneumothorax is diagnosed. c) Light index assesses pneumothorax volume $V(\%)=(1-L^3/H^3)\times100$, where L is the diameter of collapsed lung and H is the diameter of the hemithorax on a chest radiograph. d) Collins formula: $V=4.2+(4.7\times(A+B+C))$, uses three interpleural distances measured at specified points (A, B and C) to assess the volume of pneumothorax.

pneumothorax size, is operator-dependent and is not devoid of some limitations (see table 1). However, it should be noted that some studies document diagnosis of big pneumothorax on lung US when the lung point is visible in the mid-axillary line or below [65]. US shows high utility in detection of pneumothorax in supine patients, trauma patients, after lung biopsy or in the assessment prior to intercostal tube removal. CT is still a gold standard imaging modality in detecting pneumothorax. The volumetric, thin-slice (1.5 mm) technique is optimal for detection of pneumothorax and also underlying causes (such as blebs, infection or rib fracture). CT scans are performed when radiographs are difficult to interpret, differential diagnosis is needed, to detect underlying causes (*e.g.* interstitial lung disease), to rule out complications (*e.g.* extra-pleural drain position) or to drain a loculated pneumothorax. In case of doubtful situations, CT scans should be performed especially in patients with underlying lung diseases.

The diaphragm

As the primary muscle responsible for breathing, the diaphragm plays a crucial role in the respiratory process. This dome-shaped muscle separates the chest cavity from the abdominal cavity and during contraction it flattens and moves caudally, thus increasing the volume of the chest cavity, allowing the flow of air. Conversely, as the diaphragm muscle relaxes it returns to its dome shape due to the elasticity of the lungs.

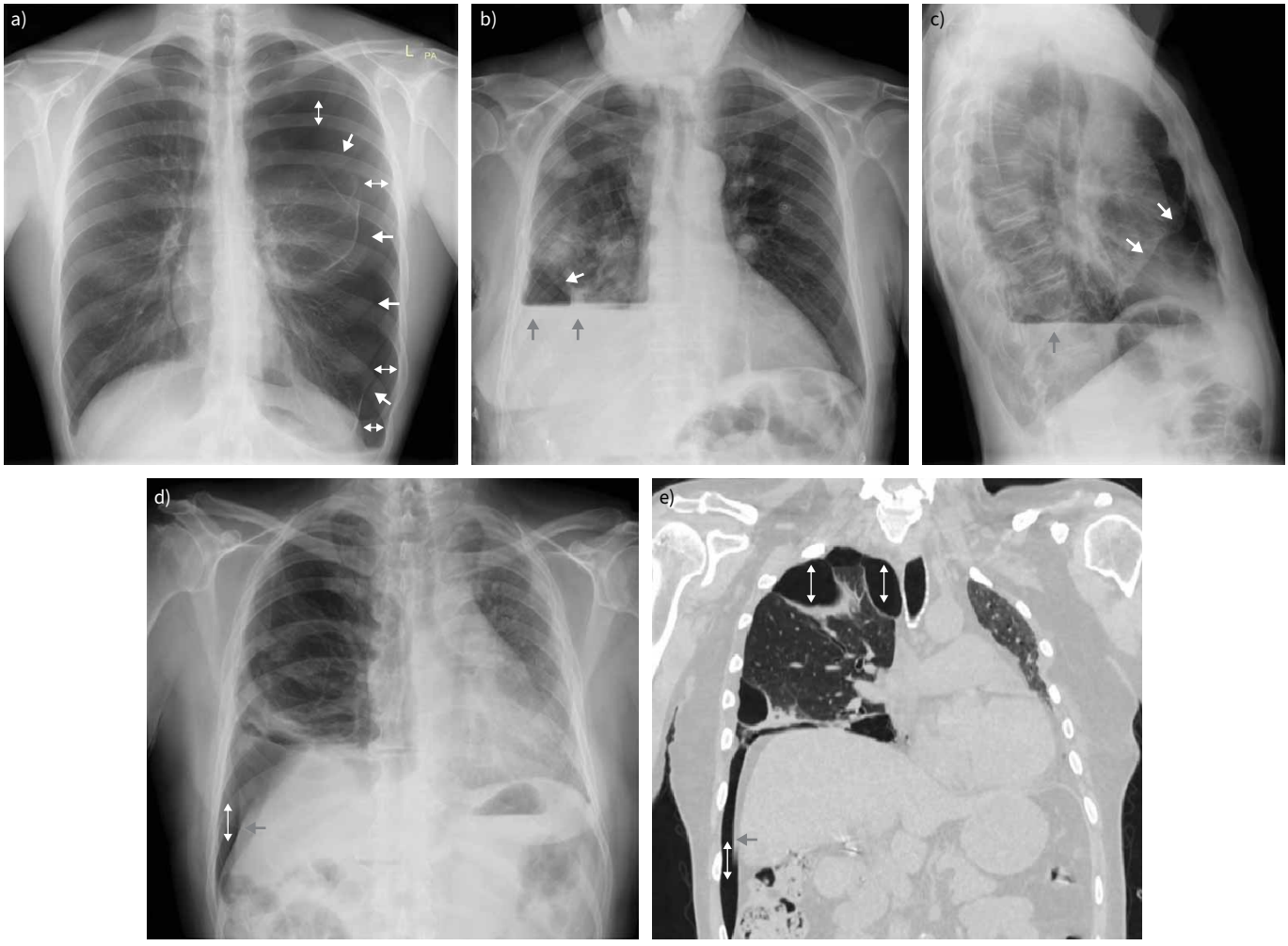

FIGURE 7 a) Upright, posterior–anterior (PA) radiograph with pneumothorax on the left side. White arrows show visceral pleura, which is a thin, sharply defined opaque (white) line with aerated lung (with visible vessels and lung tissue) on the hilar side. b) Chest radiograph PA view showing pneumothorax *ex vacuo* after pleural effusion evacuation in a patient with long-standing rheumatoid pleuritis. c) Lateral radiograph of the same patient shown in panel b. White arrows show visceral pleura of collapsed lung lobe, grey arrows show pleural effusion forming a horizontal line. d) Radiograph and e) computed tomography of the same patient with loculated pneumothorax. Thin white arrows show air in the pleural cavity. Grey arrows show deep sulcus sign.

Several diseases and conditions can affect diaphragm function, leading to impaired breathing. These include central and peripheral neurological disorders, neuromuscular, mediastinal lesions or trauma, and pulmonary diseases such as COPD, lung fibrosis or pleural effusion. Diaphragmatic dysfunction, paresis or paralysis leads to breathing difficulties ranging from mild dyspnoea during exercise to respiratory failure [66].

Imaging of diaphragm function

The most used imaging modalities to evaluate diaphragm function are fluoroscopy and US. While fluoroscopy has traditionally been used, it holds significant disadvantages compared with US, such as exposure to radiation and the lack of mobility and portability that allows US to be performed at the point of care in the emergency department, in the respiratory ward or in the intensive care unit. US can measure the excursion of the diaphragm during breathing, as well as the thickness of the muscle in contraction and relaxation.

Ultrasound modalities

Different US modalities can aid evaluation of diaphragm function. In normal B-mode, excursion of the diaphragm can be easily visualised and gross dysfunction in either of the hemidiaphragms appears. However, it may be useful to quantify contraction and for this the most used US modality is the M-mode.

TABLE 1 Conditions mimicking pneumothorax on imaging and limitations of imaging tests in diagnosis of pneumothorax

Chest radiograph	Ultrasound	CT
Skin folds artefacts: these usually have a broad edge, are opaque (white) but outlined by a sharp linear lucent (dark) line laterally, can extend beside the thoracic cavity or terminate abruptly, usually bilateral, visible distal lung markings[#]	Large bullae: sometimes lung pulse is visible, in the majority of cases CT is mandatory	Breathing artefacts
The medial border of the scapula may mimic the lung edge, but distal lung markings are visible, and while tracing the line, the shape of the scapula is present	Pleurodesis: no sliding but pleura artefacts visible	CT requires more time and resources to perform, involves a higher radiation dose, has a high cost and is more difficult to perform in some patients (*e.g.* ICU)
Large bullae: comparison with previous radiographs or internal lung markings may be helpful, in case of pneumothorax "double wall sign", sometimes compressed adjacent lung may be visible	Subcutaneous emphysema: as air accumulates in subcutaneous tissue the ribs are not visible, and there is no bat sign	
Hyperinflation may mimic the deep sulcus sign; other signs of emphysematous lung might be helpful in diagnosis[¶]	Placement of ultrasound probe parallel to the rib: it is helpful to have longitudinal probe placement and detection of the bat sign first	
Unilateral lucent lung: caused by technical factors including uneven exposure or rotation	Atelectasis: no sliding but presence of lung pulse or pleura line artefacts	
Extrathoracic gas: air in the space between parietal pleura and endothoracic fascia or mediastinum, usually a wavy line is visible; CT may be needed	Massive fibrosis: no sliding, but horizontal pleura line artefacts present	
Artefacts from clothing and linen: similar artefacts might be visible outside the thorax		

CT: computed tomography; ICU: intensive care unit. [#]: it should be noted that in normal chest radiographs, peripheral lung markings may be less prominent, especially in the upper lobes; [¶]: flattened diaphragm, frequently bilateral findings, increased anterior–posterior diameter on the lateral radiograph.

Total excursion is easily measured on the right side using the liver as an acoustic window toward the dorsal part of the diaphragm in the midclavicular line. Contraction appears as a wave shape and total excursion measured as the difference between top (contraction/inspiration) and bottom (relaxation, expiration). Furthermore, contraction and release velocity can be measured giving information on muscle strength and lung recoil conditions. In lateral positions the thickness of the diaphragm muscle gives information about contractional strength and breathing efforts as the fraction, difference or ratio between thickness in inspiration *versus* expiration [67].

Clinical utility

Non-imaging evaluation of the diaphragm includes invasive neuromuscular or oesophageal pressure measurements and are thus limited to selected patients. In intensive care medicine, US plays a role during weaning patients from mechanical ventilation setting the optimal time point for extubation. In respiratory medicine, diaphragm evaluation has been shown to relate to symptom relief following thoracentesis [68, 69]. In COPD, hyperinflation may lead to displacement of the diaphragm and muscular dysfunction may additionally reduce contractility [70]. While diaphragm dysfunction may play a role during acute exacerbation of COPD, additional studies are needed to define its place in clinical recommendations and practice, especially in relation to respiratory failure requiring noninvasive ventilation [71]. Likewise, its role in the field of interstitial lung diseases is yet to be established, but studies suggest high prevalence of diaphragm dysfunction in idiopathic pulmonary fibrosis and connective tissue disease-related interstitial lung disease.

Future directions

A pervasive problem with diaphragm evaluation is the lack of standardised methodology. Agreement on US scanning protocols needs to be set. Normal values, correlation to non-US methods and cut-off levels to rule in or out the presence of diaphragm dysfunction must be elaborated and established. Also, clinical studies on its ability to detect, monitor, predict and influence clinical decision making are needed before US evaluation is ready for the respiratory clinic.

Imaging in prediction of pleural outcomes

Imaging predictors of the outcomes of pleural intervention have been the focus of study in different disease areas and carry promise for providing noninvasive clues to direct further management particularly in MPE [6].

Non-expandable lung

The term "non-expandable lung" (NEL) encompasses a range of conditions characterised by the incapacity of the lung to undergo the expansion necessary for physiological pleural interactions. Three principal aetiologies of NEL have been identified: 1) endobronchial obstruction leading to lobar collapse or chronic lung atelectasis; 2) reduced pulmonary compliance attributable to extensive pulmonary scarring and fibrosis; and 3) constriction of the visceral pleura as a sequela to pleural pathology [72–74]. Depending on the underlying cause of visceral pleural restriction, two distinct categories of NEL have been documented: trapped lung and lung entrapment.

In patients afflicted with trapped lung, the extraction of fluid from the pleural space is concomitant with a precipitous decline in pleural pressure (P_{pl}), typically manifesting as an initially negative P_{pl} reading. Conversely, lung entrapment permits a partial re-expansion of the lung during the initial stages of pleural fluid drainage and is commonly identified by a positive baseline P_{pl}. However, when the initial pleural pressure–volume curve maintains a normal or near-normal pattern while fluid removal continues, it signifies the lung's limitation in re-expanding beyond a specific volume threshold. This phenomenon is visually represented by the steeper descent observed in the second segment of the pressure–volume curve.

Diagnosis of NEL

The identification of an NEL holds significant relevance in the decision-making process for managing patients afflicted by MPE. Depending on factors such as the patient's clinical condition, anticipated lifespan, personal preferences and the lung's capacity for re-expansion, clinicians can propose one of three therapeutic strategies: 1) serial thoracenteses, 2) pleurodesis, or 3) the insertion of an indwelling pleural catheter (IPC). Both pleurodesis and the IPC placement are regarded as "definitive" interventions [75], leading to enhanced health-related quality of life [76] and a decreased likelihood of future pleural procedures. It is imperative to assess lung expandability when contemplating pleurodesis as a treatment option, as effective pleural adhesion necessitates adequate pleural apposition.

While pleural manometry serves as an elegant technique for estimating pleural elastance and gauging the mechanical attributes of the lung, the assessment of lung expandability can also be gleaned from radiological indicators, such as visceral pleura thickening, basal pneumothorax, septated pleural effusion [77], ipsilateral volume loss, lobar atelectasis [78], pneumothorax *ex vacuo*, or inability to attain complete lung re-expansion following the removal of pleural fluid.

In a study by Chopra *et al*. [79], researchers examined the relationship between pleural elastance and post-thoracentesis radiographic findings in 70 patients with MPE. Elevated pleural elastance was seen in 51.4%, with 54% showing incomplete lung re-expansion. Only 71% showed agreement between pleural elastance and radiography; 29% had conflicting results. Normal pleural elastance correlated with 68% achieving complete lung re-expansion *versus* 25% with elevated pleural elastance. This study warns against solely relying on pleural elastance for lung expandability predictions and suggests its potential role in patient selection for pleurodesis, urging further investigation into pleurodesis outcomes.

Furthermore, some studies propose that the integration of manometry with other methods, such as lung US, can enhance its diagnostic and therapeutic utility. Salamonsen *et al*. [80] demonstrated that the incorporation of US could heighten the sensitivity in diagnosing an NEL by measuring various parameters, including the displacement of the collapsed lung during a breath hold using M-mode US.

In a study conducted on a group of 365 patients diagnosed with MPE, Trovisco *et al*. [81] demonstrate a correlation between the frequency of NEL and lung cancer as the cause of pleural fluid (70.6% of patients with NEL). Furthermore, the occurrence of NEL was higher in patients with identified loculated fluid in the pleural cavity (67% of patients with NEL).

Hassan *et al*. [82] demonstrated the capability of US to assess the displacement of the collapsed lung and its echogenicity to determine its potential for re-expansion. The comparison of lung echogenicity made against the echogenicity of the liver quantified with the assistance of software revealed the area under the curve of lung/liver echogenicity to predict NEL was 0.77 (95% CI 0.55–1; p=0.03). A cut-off of >1.6 had 71% sensitivity and 83% specificity.

Diaphragm dynamics and pleural fluid drainage

Recent studies have focused on analysing the role of the diaphragm and its function in the context of management of patients with symptomatic pleural effusion. The PLEASE-1 study, by Muruganandan *et al*. [68], focused on thoracentesis in patients with symptomatic pleural effusion. Besides demonstrating a notable improvement in breathlessness after thoracentesis, the study also presented compelling observations concerning the diaphragm. Pre-drainage, 50% had altered diaphragm dynamics on US, which mostly normalised afterwards. Regardless of the initial condition, most experienced improved breathlessness and diaphragm movement. A significant link ($p<0.001$) was found between movement and effusion appearance. After drainage, those with normalised diaphragm shape often regained normal movement. Post-drainage, 73% of all participants showed improved breathlessness; notably, 84% of NEL patients exhibited meaningful improvement.

Based on the findings regarding diaphragm function in the PLEASE-1 study, the researchers initiated an investigation to examine the impact of pleural effusion on the function of both hemidiaphragms. Data from the pilot PLEASE-2 study suggest that unilateral pleural effusions affect the function of both hemidiaphragms [83]. Moreover, it has been noted that the abnormal function of the ipsilateral and contralateral of both hemidiaphragms resolved post-drainage.

Ultrasound and pleurodesis outcome

Pleurodesis is a medical or surgical procedure that involves applying one or more of various injurious agents between the visceral and parietal and pleural membranes with the aim of inducing pleural symphysis and preventing re-accumulation of fluid (air or liquid) in the space [14]. Pleural symphysis will invariably cause cessation of pleural sliding, a sign that can be seen on pleural US [6]. The cessation of pleural sliding on US following pleurodesis was first demonstrated in a surgical cohort of patients who underwent mechanical pleurodesis (*via* pleural abrasions) for pneumothorax [84]. In an animal model of pleurodesis, the lack of sliding on US strongly correlated with the presence of macroscopic and microscopic pleural adhesions [85]. In a case series of patients with MPE undergoing talc slurry pleurodesis, the adherence score (a composite of scores in different zones of the hemithorax based on whether sliding was present) measured 24 h after talc administration correlated with the risk of pleurodesis failure [86]. In a multicentre trial of patients with MPE undergoing pleurodesis, using the adherence score as opposed to the standard of care (chest radiograph findings plus pleural fluid output) led to shorter hospital stays and was found to be highly cost-effective [87]. In a small case series, the presence of echogenic swirling patterns in patients with MPE was associated with higher risk of subsequent talc pleurodesis failure [88].

Endoscopy

In essence, thoracoscopy is the ultimate imaging test for the pleura. It provides access to the pleural space allowing direct visualisation of the visceral and parietal pleurae. According to the approach, the procedure can be carried out in spontaneously breathing patients (medical thoracoscopy) or under general anaesthesia (thoracoscopic surgery) and can be achieved *via* one, two or three ports according to the complexity of the intervention intended [89].

In cases where pleural effusion is present, complete evacuation of the space is attempted first to optimise examination. It is normally feasible to examine the full costal pleura and diaphragmatic pleura as well as the visceral pleura overlying the lung surfaces. It is also technically feasible to examine the pericardium [90].

Normally, the parietal pleura appears pink, shiny and smooth and the neurovascular bundle as well as subpleural adipose tissue can be easily appreciated (figure 8a). Certain findings are regarded as strongly suggestive of malignancy or specific inflammation (*i.e.* tuberculosis); however, in all cases parietal pleural biopsies are carried out to confirm diagnosis and obtain tissue for ancillary pathological, genetic or microbiological testing. In comparison to thoracoscopic biopsies as the golden standard test, Hallifax *et al.* [11] demonstrated that pre-thoracoscopy CT scans have a sensitivity of 68% for pleural malignancy.

The presence of large nodules or masses is diagnostic of pleural malignancy (figure 8b). In some cases of pleural malignancy, particularly in mesothelioma, the predominant abnormality is diffuse thickening obscuring the normal anatomy. In PTB, diffuse micronodularity (likened to “sago pudding” due to the distinct pearly tuberculomas) can be highly suggestive of the diagnosis (figure 8c) [91].

In a substantial proportion of patients, diffuse thickening with inflammation is noted with no obvious nodularity. Some of these cases end up having malignancy on biopsy, but others have nonspecific fibrosis/inflammation. Several technologies have been explored to enhance the identification of pleural

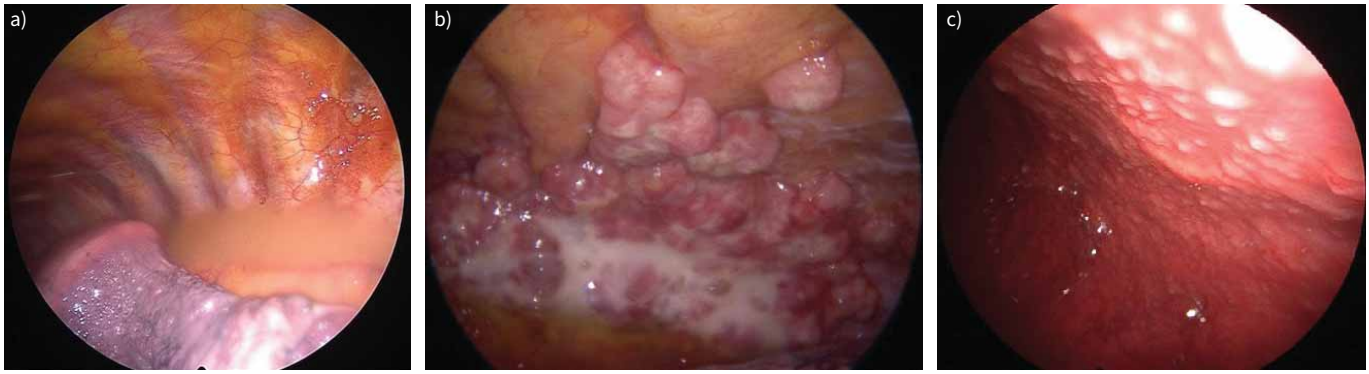

FIGURE 8 Thoracoscopic images of a) parietal pleural inflammation (note the prominent vasculature), b) malignant pleural nodularity, and c) the "sago pudding" appearance in pleural tuberculosis. Images courtesy of Gian Pietro Marchetti (Spedali Civili di Brescia, Brescia, Italy).

abnormalities beyond using white light in such cases. Narrow-band imaging (which uses specific wave lengths of light with different absorption capabilities) improves visualisation of irregular vascular patterns, a feature of pleural malignancy [92]. More recently, optical coherence tomography (OCT), an imaging technique that utilises infra-red light and which is commonly used in ophthalmology to provide high-definition images of the retina and optic nerve, has been adapted in the form of a probe that be can used *via* thoracoscopy. In an animal model, OCT was able to supply tissue-level images of the pleura [93].

Another technique that has shown promise in providing highly magnified *in vivo* micrographs of the pleura is confocal laser endomicroscopy, which involves intravenous injection of fluorescein, followed by probe-based examination of the pleura producing real-time examination of pleural tissue. This novel tool could successfully differentiate pleural fibrosis from pleural malignancy with reasonable inter-rater agreement [94].

Newer tools in imaging the pleura

Contrast-enhanced ultrasound and ultrasound elastography

US examination is a widely used modality not only among radiologists but also among general physicians due to ease of use, accessibility, robust diagnostic utility, high safety and low cost. Furthermore, recent advancements in this imaging modality, such as contrast-enhanced US (CEUS), have shown promise in combining superior temporal and spatial resolution with real-time dynamic enhancement. This has led to a surge in interest in the use of CEUS in both diagnostic and interventional procedures, particularly in paediatric radiology. CEUS is an advanced US technique in which microbubble contrast agents like sulfur hexafluoride lipid-type A microspheres are injected intravascularly for a better characterisation of lesions [95]. YANG *et al*. [96] conducted a study demonstrating that high-frequency B-mode US, in conjunction with CEUS, can effectively differentiate between benign and malignant pleural lesions.

In interventional radiology, US contrast agents can be administered intravenously or intracavitary. Intravenous CEUS applications can improve lesion detection and differentiate between solid enhancing components and non-enhancing areas, such as necrotic or cystic regions, thereby improving the diagnostic confidence of US-guided pleural biopsies [97, 98]. For procedures guided by US, such as the drainage of pleural abscesses or empyema, intracavitary contrast agents can be invaluable in assessing drain positioning and characterising abscess formations, including features like multilocularity [97]. A promising application of CEUS is the intracavitary application of the contrast agent to detect a peritoneal–pleural communication [99].

However, it is important to note that the use of CEUS for characterising pleural lesions is still in the experimental phase and has not yet gained widespread adaptation in clinical practice. Further research and clinical validation are needed to fully integrate this innovative approach into routine medical practice.

Besides CEUS, US elastography is another promising US application for the evaluation of pleural processes [100, 101]. Elastography is a novel US technology already used routinely to evaluate breast and thyroid lesions as well as liver tissue to assess tissue stiffness [100]. US elastography allows for the assessment of tissue stiffness by quantifying the tissue's response to mechanical stress. This stress is

generated either by compression stimuli or by shear waves [102]. Recently published studies indicate that US elastography may be a valuable tool to differentiate MPM or pleural metastases from benign processes [100, 103, 104]. Furthermore, US elastography has been reported in several studies to increase the diagnostic yield of US-guided pleural biopsies [101, 105]. In a multicentre study including 98 patients, Deng *et al*. [105] demonstrated that it is possible to reach a diagnostic yield for pleural biopsies of 92.9% using US elastography. However, US elastography is an operator-dependent method [102], and more studies are needed to demonstrate its general usability. Furthermore, US elastography measurements are vendor-specific and may vary from one US device to another. Finally, since the safety of US elastography is not well investigated, its use should be limited to the region of interest, and direct exposure of the pleura should be avoided [106].

Novel PET tracers for the evaluation of pleural tumours

While fluorodeoxyglucose (FDG) is widely used for the evaluation of patients with suspected or known malignancies and some inflammatory diseases, the interpretation of FDG-PET studies is impaired by the low specificity of this tracer. In short, a high FDG uptake indicates a high glucose uptake, which is not only observed in malignant tumours but is also observed in several benign processes. Consequently, FDG-PET CT suffers from a high false-positive rate. To overcome this problem, several more specific PET tracers have been developed over the past few years.

Of these tracers, FAPI is of particular interest in oncology. FAPI, a radiolabelled fibroblast activation protein inhibitor, binds specifically to the fibroblast activation protein (FAP), which is a transmembrane glycoprotein that is overexpressed by fibroblasts of the tumour stroma [107]. FAPI-PET CT has been shown to be a promising tracer for the evaluation of several tumours, such as lung cancer, primary hepatic tumours, pancreatic ductal adenocarcinoma and gastrointestinal tumours [107]. Early small studies and case reports indicate that FAPI might be superior to FDG for the diagnosis and staging of fibroblastic tumours such as the solitary fibrous tumour of the pleura (SFPT) [108, 109].

Another study explored the feasibility of PET-CT using the newer tracer gallium-68 (^{68}Ga)-pentixafor to noninvasively assess CXCR4 expression in pleural mesothelioma [110]. These emerging tracers hold great potential for addressing the current limitations of PET-CT in oncological imaging and may significantly enhance our ability to diagnose and understand malignant tumours, particularly in challenging cases like mesothelioma.

Another potential novel tracer for the diagnosis of SFPTs is ^{68}Ga-DOTATOC, which binds specifically to somatostatin receptor subtype 2. ^{68}Ga-DOTATOC is primarily used for the diagnosis and staging of neuroendocrine tumours, which show a high expression of this receptor, as well as for the diagnosis of meningiomas [111, 112]. Anecdotal cases of patients with SFPTs indicate that ^{68}Ga-DOTATOC might also be used for the diagnosis of the tumour as well as for the detection of recurrence [113, 114].

Dynamic contrast and diffusion MRI and PET-MRI

An alternative approach to overcome the limitations of PET-CT is the use of MRI. MRI is the first modality for characterisation of a pleural lesion, local staging of the malignant tumour and distinguishing between malignant and benign tumours. Previously, MRI was underutilised in lung imaging due to two significant disadvantages: a low signal-to-noise ratio in lung tissues and susceptibility artefacts resulting from air, as well as cardiac and respiratory motion. However, the adoption of free-breathing diffusion-weighted imaging (DWI) and volumetric interpolated breath-hold examination (VIBE) sequences for dynamic contrast-enhanced (DCE) imaging can significantly improve accuracy and specificity in differentiating malignant pleural tumours from benign lesions in comparison to PET-CT, and correct false-positive findings on PET-CT scans triggered by inflammation or talc pleurodesis [115].

Continuous advancements in technology have led to the development of a new generation of MRI scanners, making them increasingly practical for routine medical use. The latest creation in hybrid machines is a machine which combines both PET and MRI capabilities to achieve the high soft tissue resolution of MRI with the functional information about metabolic activity from PET. PET-MRI represents a promising modality with the potential to provide comprehensive and thorough assessments of both local and distant tumour staging. A study by Murphy *et al*. [116] revealed that PET-MRI provides more accurate locoregional staging, particularly in T-staging, compared with PET-CT, while achieving equivalent results in N-staging. The main limitation of the PET-MRI examination is the high cost of the machine and the individual study itself, with a relatively long examination time. Additionally, there are other contraindications, such as the presence of a pacemaker or the patient's critical medical conditions, that may restrict the feasibility of this imaging modality.

Key points

- Both CT and US have superior sensitivity in detecting pleural effusion in comparison to chest radiography and are able to reveal only few millilitres of pleural fluid.
- US is more sensitive in revealing pleural fluid septations, but mediastinal pockets of pleural fluid can only be visualised *via* CT.
- Mesothelioma imaging is challenging because of complex morphology and low disease volume at first presentation. Multiple modalities are needed for accurate assessment, with CT and US being the foremost in most patients.
- In the setting of MPE, the identification of NEL is crucial for planning management and enabling the selection of an appropriate therapeutic approach.
- In pneumothorax, CT scans are performed when chest radiographs are difficult to interpret, differential diagnosis is needed, to detect underlying causes (*e.g.* interstitial lung disease), to rule out complications (*e.g.* extra-pleural drain position) or to drain a loculated pneumothorax.
- US can easily evaluate diaphragm excursion and contractility and allows bed-side examinations in multiple clinical settings.

Self-evaluation questions

1. US scanning is least useful in the examination of:
    a) Pneumothorax
    b) Pleural fluid septation
    c) Intercostal vessels
    d) Mediastinal fluid pockets
    e) Diaphragm mobility
2. The following is/are true regarding diaphragm dysfunction:
    a) Diaphragm dysfunction occurs as a problem in peripheral neurological disorders only
    b) Diaphragm dysfunction can be assessed by fluoroscopy and US
    c) Symptoms of diaphragm dysfunction include shortness of breath and respiratory failure
    d) US evaluation of the diaphragm is easily performed; include standard projections and follow a specific protocol
3. The feature not consistent with pleural infection on chest CT is:
    a) Split pleural sign
    b) Hypertrophy of the extra-pleural fat
    c) Pleural nodularity
    d) Ipsilateral consolidation
    e) Pleural enhancement

Conflicts of interest: The authors have no conflicts of interest to declare in relation to the subject of this work.

References

1 Noppen M. Normal volume and cellular contents of pleural fluid. *Curr Opin Pulm Med* 2001; 7: 180–182.
2 Duerden L, Benamore R, Edey A. Radiology in pleural disease: what is the role of chest radiographs, CT and PET in modern management? *In*: Maskell NA, Laursen CB, Lee YCG, Rahman NM, eds. Pleural Disease (ERS Monograph). Sheffield, European Respiratory Society, 2020; pp. 48–72.
3 Pairon J-C, Laurent F, Rinaldo M, *et al.* Pleural plaques and the risk of pleural mesothelioma. *J Natl Cancer Inst* 2013; 105: 293–301.
4 Colins JD, Burwell D, Furmanski S, *et al.* Minimal detectable pleural effusions. A roentgen pathology model. *Radiology* 1972; 105: 51–53.
5 Brixey AG, Luo Y, Skouras V, *et al.* The efficacy of chest radiographs in detecting parapneumonic effusions. *Respirology* 2011; 16: 1000–1004.
6 Hassan M, Mercer RM, Rahman NM. Thoracic ultrasound in the modern management of pleural disease. *Eur Respir Rev* 2020; 29: 190136.
7 Clive AO, Jones HE, Bhatnagar R, *et al.* Interventions for the management of malignant pleural effusions: a network meta-analysis. *Cochrane Database Syst Rev* 2016; 5: CD010529.
8 Clive AO, Kahan BC, Hooper CE, *et al.* Predicting survival in malignant pleural effusion: development and validation of the LENT prognostic score. *Thorax* 2014; 69: 1098–1104.
9 Hassan M, Mercer RM, Maskell NA, *et al.* Survival in patients with malignant pleural effusion undergoing talc pleurodesis. *Lung Cancer* 2019; 137: 14–18.
10 Leung AN, Müller NL, Miller RR. CT in differential diagnosis of diffuse pleural disease. *AJR Am J Roentgenol* 1990; 154: 487–492.

11 Hallifax RJ, Haris M, Corcoran JP, *et al.* Role of CT in assessing pleural malignancy prior to thoracoscopy. *Thorax* 2015; 70: 192–193.
12 Qureshi NR, Rahman NM, Gleeson FV. Thoracic ultrasound in the diagnosis of malignant pleural effusion. *Thorax* 2009; 64: 139–143.
13 Roberts ME, Rahman NM, Maskell NA, *et al.* British Thoracic Society Guideline for pleural disease. *Thorax* 2023; 78: Suppl. 3, s1–s42.
14 Mercer RM, Hassan M, Rahman NM. The role of pleurodesis in respiratory diseases. *Expert Rev Respir Med* 2018; 12: 323–334.
15 Baas P, Scherpereel A, Nowak AK, *et al.* First-line nivolumab plus ipilimumab in unresectable malignant pleural mesothelioma (CheckMate 743): a multicentre, randomised, open-label, phase 3 trial. *Lancet* 2021; 397: 375–386.
16 Katz SI, Straus CM, Roshkovan L, *et al.* Considerations for imaging of malignant pleural mesothelioma: a consensus statement from the international mesothelioma interest group. *J Thorac Oncol* 2023; 18: 278–298.
17 Metintas M, Ucgun I, Elbek O, *et al.* Computed tomography features in malignant pleural mesothelioma and other commonly seen pleural diseases. *Eur J Radiol* 2002; 41: 1–9.
18 Tsim S, Stobo DB, Alexander L, *et al.* The diagnostic performance of routinely acquired and reported computed tomography imaging in patients presenting with suspected pleural malignancy. *Lung Cancer* 2017; 103: 38–43.
19 Patel A, Roshkovan L, McNulty S, *et al.* Delayed-phase enhancement for evaluation of malignant pleural mesothelioma on computed tomography: a prospective cohort study. *Clin Lung Cancer* 2021; 22: 210–217.e1.
20 Tsim S, Humphreys CA, Cowell GW, *et al.* Early contrast enhancement: a novel magnetic resonance imaging biomarker of pleural malignancy. *Lung Cancer* 2018; 118: 48–56.
21 Grogan DR, Irwin RS, Channick R, *et al.* Complications associated with thoracentesis. A prospective, randomized study comparing three different methods. *Arch Intern Med* 1990; 150: 873–877.
22 Weingardt JP, Guico RR, Nemcek AA, *et al.* Ultrasound findings following failed, clinically directed thoracenteses. *J Clin Ultrasound* 1994; 22: 419–426.
23 Qureshi NR, Gleeson FV. Imaging of pleural disease. *Clin Chest Med* 2006; 27: 193–213.
24 Knuuttila A, Kivisaari L, Kivisaari A, *et al.* Evaluation of pleural disease using MR and CT. With special reference to malignant pleural mesothelioma. *Acta Radiol* 2001; 42: 502–507.
25 Plathow C, Staab A, Schmaehl A, *et al.* Computed tomography, positron emission tomography, positron emission tomography/computed tomography, and magnetic resonance imaging for staging of limited pleural mesothelioma: initial results. *Invest Radiol* 2008; 43: 737–744.
26 Sørensen JB, Ravn J, Loft A, *et al.* Preoperative staging of mesothelioma by 18F-fluoro-2-deoxy-D-glucose positron emission tomography/computed tomography fused imaging and mediastinoscopy compared to pathological findings after extrapleural pneumonectomy. *Eur J Cardiothorac Surg* 2008; 34: 1090–1096.
27 Lim E, Waller D, Lau K, *et al.* MARS 2: A Multicentre Randomised Trial Comparing (Extended) Pleurectomy Decortication versus No Radical Surgery for Mesothelioma. Singapore, 2023 World Conference on Lung Cancer, 9–12 September 2023. https://cattendee.abstractsonline.com/meeting/10925/Session/3
28 Armato SG, Nowak AK, Francis RJ, *et al.* Observer variability in mesothelioma tumor thickness measurements: defining minimally measurable lesions. *J Thorac Oncol* 2014; 9: 1187–1194.
29 Mozley PD, Bendtsen C, Zhao B, *et al.* Measurement of tumor volumes improves RECIST-based response assessments in advanced lung cancer. *Transl Oncol* 2012; 5: 19–25.
30 Frauenfelder T, Tutic M, Weder W, *et al.* Volumetry: an alternative to assess therapy response for malignant pleural mesothelioma? *Eur Respir J* 2011; 38: 162–168.
31 Gill RR, Naidich DP, Mitchell A, *et al.* North American multicenter volumetric CT study for clinical staging of malignant pleural mesothelioma: feasibility and logistics of setting up a quantitative imaging study. *J Thorac Oncol* 2016; 11: 1335–1344.
32 Kidd AC, Anderson O, Cowell GW, *et al.* Fully automated volumetric measurement of malignant pleural mesothelioma by deep learning AI: validation and comparison with modified RECIST response criteria. *Thorax* 2022; 77: 1251–1259.
33 Bedawi EO, Ricciardi S, Hassan M, *et al.* ERS/ESTS statement on the management of pleural infection in adults. *Eur Respir J* 2022; 61: 2201062.
34 Davies HE, Davies RJO, Davies CWH, *et al.* Management of pleural infection in adults: British Thoracic Society pleural disease guideline 2010. *Thorax* 2010; 65: Suppl. 2, ii41–ii53.
35 Bryant RE, Salmon CJ. Pleural empyema. *Clin Infect Dis* 1996; 22: 747–764.
36 Kearney SE, Davies CW, Davies RJ, *et al.* Computed tomography and ultrasound in parapneumonic effusions and empyema. *Clin Radiol* 2000; 55: 542–547.
37 Arenas-Jiménez J, Alonso-Charterina S, Sánchez-Payá J, *et al.* Evaluation of CT findings for diagnosis of pleural effusions. *Eur Radiol* 2000; 10: 681–690.
38 Hassan M, Asciak R, Rizk R, *et al.* Lung abscess or empyema? Taking a closer look. *Thorax* 2018; 73: 887–889.

39 Kearney SE, Davies CW, Tattersall DJ, *et al.* The characteristics and significance of thoracic lymphadenopathy in parapneumonic effusion and empyema. *Br J Radiol* 2000; 73: 583–587.
40 Tobin CL, Porcel JM, Wrightson JM, *et al.* Diagnosis of pleural infection: state-of-the-art. *Curr Respir Care Rep* 2012; 1: 101–110.
41 Gopi A, Madhavan SM, Sharma SK, *et al.* Diagnosis and treatment of tuberculous pleural effusion in 2006. *Chest* 2007; 131: 880–889.
42 Frye MD, Pozsik CJ, Sahn SA. Tuberculous pleurisy is more common in AIDS than in non-AIDS patients with tuberculosis. *Chest* 1997; 112: 393–397.
43 Seibert AF, Haynes J, Middleton R, *et al.* Tuberculous pleural effusion. *Chest* 1991; 99: 883–886.
44 Marjani M, Yousefzadeh A, Baghaei P, *et al.* Impact of HIV infection on tuberculous pleural effusion. *Int J STD AIDS* 2016; 27: 363–369.
45 Koegelenberg CFN, Diacon AH. Image-guided pleural biopsy. *Curr Opin Pulm Med* 2013; 19: 368–373.
46 Chen H-J, Hsu W-H, Tu C-Y, *et al.* Sonographic septation in lymphocyte-rich exudative pleural effusions: a useful diagnostic predictor for tuberculosis. *J Ultrasound Med* 2006; 25: 857–863.
47 Zhou S, Zhao J, Song X, *et al.* Imaging manifestations of B-mode ultrasound combined with CT in tuberculous pleuritis patients and the diagnostic value. *Exp Ther Med* 2018; 16: 2343–2348.
48 Levi G, Rocchetti C, Mei F, *et al.* Diagnostic role of internal mammary lymph node involvement in tuberculous pleurisy: a multicenter study. *Pulmonology* 2022; in press [https://doi.org/10.1016/j.pulmoe.2022.01.010].
49 Montuori M, Casella F, Casazza G, *et al.* Lung ultrasonography in pulmonary tuberculosis: a pilot study on diagnostic accuracy in a high-risk population. *Eur J Intern Med* 2019; 66: 29–34.
50 Akhan O, Demirkazik FB, Ozmen MN, *et al.* Tuberculous pleural effusions: ultrasonic diagnosis. *J Clin Ultrasound* 1992; 20: 461–465.
51 Elyashiv D, Alpert EA, Granat N. Empyema necessitans diagnosed by point-of-care ultrasound. *J Emerg Med* 2020; 59: e221–e223.
52 Kim JS, Shim SS, Kim Y, *et al.* Chest CT findings of pleural tuberculosis: differential diagnosis of pleural tuberculosis and malignant pleural dissemination. *Acta Radiol* 2014; 55: 1063–1068.
53 Shaw JA, Koegelenberg CFN. Pleural tuberculosis. *Clin Chest Med* 2021; 42: 649–666.
54 Song JW, Im JG, Goo JM, *et al.* Pseudochylous pleural effusion with fat-fluid levels: report of six cases. *Radiology* 2000; 216: 478–480.
55 Ebrahimi A, Yousefifard M, Mohammad Kazemi H, *et al.* Diagnostic accuracy of chest ultrasonography *versus* chest radiography for identification of pneumothorax: a systematic review and meta-analysis. *Tanaffos* 2014; 13: 29–40.
56 Kirkpatrick AW, Sirois M, Laupland KB, *et al.* Hand-held thoracic sonography for detecting post-traumatic pneumothoraces: the Extended Focused Assessment with Sonography for Trauma (EFAST). *J Trauma* 2004; 57: 288–295.
57 Dahmarde H, Parooie F, Salarzaei M. Accuracy of ultrasound in diagnosis of pneumothorax: a comparison between neonates and adults – a systematic review and meta-analysis. *Can Respir J* 2019; 2019: 5271982.
58 Butler H, Chrisanthopoulos V, Harous A, *et al.* A scoping review of clinical practice guidelines for the diagnosis of primary spontaneous pneumothorax. *J Med Imaging Radiat Sci* 2022; 53: 728–736.
59 Seow A, Kazerooni EA, Pernicano PG, *et al.* Comparison of upright inspiratory and expiratory chest radiographs for detecting pneumothoraces. *AJR Am J Roentgenol* 1996; 166: 313–316.
60 Beres RA, Goodman LR. Pneumothorax: detection with upright *versus* decubitus radiography. *Radiology* 1993; 186: 19–22.
61 Kanne JP, Rother MDM. Pneumothorax: imaging diagnosis and etiology. *Semin Roentgenol* 2023; 58: 440–453.
62 Klein JS, Brant WE, Helms CA, *et al.* Brant and Helms Podstawy Diagnostyki Radiologicznej. T. 3. 2. wydanie polskie. [Brant and Helms' Fundamentals of Diagnostic Radiology. Vol. 3. 2nd Polish Edn.] Warsaw, Medipage, 2020.
63 MacDuff A, Arnold A, Harvey J, *et al.* Management of spontaneous pneumothorax: British Thoracic Society Pleural Disease Guideline 2010. *Thorax* 2010; 65: Suppl. 2, ii18–ii31.
64 Salazar AJ, Aguirre DA, Ocampo J, *et al.* Evaluation of three pneumothorax size quantification methods on digitized chest X-ray films using medical-grade grayscale and consumer-grade color displays. *J Digit Imaging* 2014; 27: 280–286.
65 Volpicelli G, Boero E, Sverzellati N, *et al.* Semi-quantification of pneumothorax volume by lung ultrasound. *Intensive Care Med* 2014; 40: 1460–1467.
66 Pałac M, Rutka M, Wolny T, *et al.* Ultrasonography in assessment of respiratory muscles function: a systematic review. *Respiration* 2022; 101: 878–892.
67 Ferrari G, Helbo Skaarup S, Panero F, *et al.* The diaphragm. *In*: Laursen CB, Rahman NM, Volpicelli G, eds. Thoracic Ultrasound (ERS Monograph). Sheffield, European Respiratory Society, 2018; pp. 129–147.
68 Muruganandan S, Azzopardi M, Thomas R, *et al.* The Pleural Effusion And Symptom Evaluation (PLEASE) study of breathlessness in patients with a symptomatic pleural effusion. *Eur Respir J* 2020; 55: 1900980.

69 Skaarup SH, Lonni S, Quadri F, *et al.* Ultrasound evaluation of hemidiaphragm function following thoracentesis: a study on mechanisms of dyspnea related to pleural effusion. *J Bronchology Interv Pulmonol* 2020; 27: 172–178.

70 Hua-Rong Z, Liang C, Rong L, *et al.* Ultrasonographic evaluation of diaphragm function in patients with chronic obstructive pulmonary disease: a systematic review and meta-analysis. *Medicine (Baltimore)* 2022; 101: e32560.

71 Kocyigit H, Gunalp M, Genc S, *et al.* Diaphragm dysfunction detected with ultrasound to predict noninvasive mechanical ventilation failure: a prospective cohort study. *Am J Emerg Med* 2021; 45: 202–207.

72 Grabczak EM, Krenke R. Pleural interventions: manometry. *In*: Janes SM, ed. Encyclopedia of Respiratory Medicine. Cambridge, Academic Press, 2022; pp. 544–565.

73 Hu K, Chopra A, Huggins JT, *et al.* Pleural manometry: techniques, applications, and pitfalls. *J Thorac Dis* 2020; 12: 2759–2770.

74 Huggins JT, Maldonado F, Chopra A, *et al.* Unexpandable lung from pleural disease. *Respirology* 2018; 23: 160–167.

75 Bibby AC, Dorn P, Psallidas I, *et al.* ERS/EACTS statement on the management of malignant pleural effusions. *Eur Respir J* 2018; 52: 1800349.

76 Sivakumar P, Saigal A, Ahmed L. Quality of life after interventions for malignant pleural effusions: a systematic review. *BMJ Support Palliat Care* 2020; 10: 45–54.

77 Thomas R, Jenkins S, Eastwood PR, *et al.* Physiology of breathlessness associated with pleural effusions. *Curr Opin Pulm Med* 2015; 21: 338–345.

78 Heidecker JT, Huggins JT, Doelken P, *et al.* Pre- and postthoracentesis chest radiographic findings do not predict abnormal pleural elastance. *Chest* 2006; 130: Suppl., 244S.

79 Chopra A, Judson MA, Doelken P, *et al.* The relationship of pleural manometry with postthoracentesis chest radiographic findings in malignant pleural effusion. *Chest* 2020; 157: 421–426.

80 Salamonsen MR, Lo AKC, Ng ACT, *et al.* Novel use of pleural ultrasound can identify malignant entrapped lung prior to effusion drainage. *Chest* 2014; 146: 1286–1293.

81 Trovisco R, Freitas C, Serino M, *et al.* Predictors of lung entrapment in malignant pleural effusion. *Pulmonology* 2022; in press [https://doi.org/10.1016/j.pulmoe.2022.08.001].

82 Hassan M, El-Shaarawy B, Al-Qaradawi MY, *et al.* Ultrasound predictors of lung re-expansion following pleural effusion drainage. *Eur Respir J* 2021; 58: Suppl. 65, OA4342.

83 Fitzgerald DB, Muruganandan S, Peddle-McIntyre CJ, *et al.* Ipsilateral and contralateral hemidiaphragm dynamics in symptomatic pleural effusion: the 2nd PLeural Effusion And Symptom Evaluation (PLEASE-2) Study. *Respirology* 2022; 27: 882–889.

84 Leo F, Dellamonica J, Venissac N, *et al.* Can chest ultrasonography assess pleurodesis after VATS for spontaneous pneumothorax? *Eur J Cardiothorac Surg* 2005; 28: 47–49.

85 Tazi-Mezalek R, Frankel D, Fortin M, *et al.* Chest ultrasonography to assess the kinetics and efficacy of talc pleurodesis in a model of pneumothorax: an experimental animal study. *ERJ Open Res* 2018; 4: 00158-2017.

86 Corcoran JP, Hallifax RJ, Mercer RM, *et al.* Thoracic ultrasound as an early predictor of pleurodesis success in malignant pleural effusion. *Chest* 2018; 154: 1115–1120.

87 Psallidas I, Hassan M, Yousuf A, *et al.* Role of thoracic ultrasonography in pleurodesis pathways for malignant pleural effusions (SIMPLE): an open-label, randomised controlled trial. *Lancet Respir Med* 2021; 10: 139–148.

88 Hassan M, Asciak R, Mercer RM, *et al.* Echogenic swirling seen on ultrasound and outcome of pleurodesis in malignant pleural effusion. *Arch Bronconeumol* 2019; 55: 659–661.

89 Pinelli V, Clive AO. Medical thoracoscopy in 2020: essential and future techniques. *In*: Maskell NA, Laursen CB, Lee YCG, Rahman NM, eds. Pleural Disease (ERS Monograph). Sheffield, European Respiratory Society, 2020; pp. 120–137.

90 Loddenkemper R, Lee P, Noppen M, *et al.* Medical thoracoscopy/pleuroscopy: step by step. *Breathe* 2011; 8: 156–167.

91 Shaw JA, Ahmed L, Koegelenberg CFN. Effusions related to TB. *In*: Maskell NA, Laursen CB, Lee YCG, Rahman NM, eds. Pleural Disease (ERS Monograph). Sheffield, European Respiratory Society, 2020; pp. 172–192.

92 Schönfeld N, Schwarz C, Kollmeier J, *et al.* Narrow band imaging (NBI) during medical thoracoscopy: first impressions. *J Occup Med Toxicol* 2009; 4: 24.

93 Xie T, Liu G, Kreuter K, *et al. In vivo* three-dimensional imaging of normal tissue and tumors in the rabbit pleural cavity using endoscopic swept source optical coherence tomography with thoracoscopic guidance. *J Biomed Opt* 2009; 14: 064045.

94 Wijmans L, Baas P, Sieburgh TE, *et al.* Confocal laser endomicroscopy as a guidance tool for pleural biopsies in malignant pleural mesothelioma. *Chest* 2019; 156: 754–763.

95 Malone CD, Fetzer DT, Monsky WL, *et al.* Contrast-enhanced US for the interventional radiologist: current and emerging applications. *Radiographics* 2020; 40: 562–588.

96 Yang H, Zhang Y, Wei D, *et al.* Utility of high-frequency B-mode and contrast-enhanced ultrasound for the differential diagnosis of benign and malignant pleural diseases: a prospective study. *J Thorac Dis* 2022; 14: 3695–3705.

97 Acord MR, Cahill AM, Durand R, *et al.* Contrast-enhanced ultrasound in pediatric interventional radiology. *Pediatr Radiol* 2021; 51: 2396–2407.

98 Sun W, Zhou Y, Yang C, *et al.* Contrast-enhanced ultrasound guided pleural biopsy improves diagnostic confidence for pleural based lesions: a 3-year prospective study. *BMC Pulm Med* 2021; 21: 224.

99 Sidhu PS, Cantisani V, Dietrich CF, *et al.* The EFSUMB guidelines and recommendations for the clinical practice of contrast-enhanced ultrasound (CEUS) in non-hepatic applications: update 2017 (Short Version). *Ultraschall Med* 2018; 39: 154–180.

100 Jiang B, Li X, Yin Y, *et al.* Ultrasound elastography: a novel tool for the differential diagnosis of pleural effusion. *Eur Respir J* 2019; 54: 1802018.

101 Zhang Q, Deng M-M, Li X-L, *et al.* Thoracic ultrasound-guided real-time pleural biopsy in the diagnosis of pleural diseases: a systematic review and meta-analysis. *Expert Rev Respir Med* 2023; 17: 805–813.

102 Porcel JM. Ultrasound-based elastography: "hard" to implement in the pleural effusion work-up? *Eur Respir J* 2019; 54: 1901587.

103 Ozgokce M, Yavuz A, Akbudak I, *et al.* Usability of transthoracic shear wave elastography in differentiation of subpleural solid masses. *Ultrasound Q* 2018; 34: 233–237.

104 Jiang B, Li X, Yin Y, *et al.* Pleural ultrasound elastography: a novel technique for the differential diagnosis of malignant pleural effusion. *SSRN* 2018; preprint [https://doi.org/10.2139/ssrn.3267681].

105 Deng M, Ye X, Ma J, *et al.* Ultrasonic elastography-guided pleural biopsy for the diagnosis of pleural effusion: a multicenter prospective study of diagnostic test performance. *Annals ATS* 2023; 20: 1242–1249.

106 Wolfram F, Miller D, Demi L, *et al.* Best practice recommendations for the safe use of lung ultrasound. *Ultraschall Med* 2023; 44: 516–519.

107 Chandekar KR, Prashanth A, Vinjamuri S, *et al.* FAPI PET/CT imaging – an updated review. *Diagnostics (Basel)* 2023; 13: 2018.

108 Zhang A, Meng X, Yao Y, *et al.* Head-to-head assessment of [^{68}Ga]Ga-DOTA-FAPI-04 PET/CT *vs* [^{18}F]FDG PET/CT in fibroblastic tumors. *Eur J Radiol* 2022; 155: 110507.

109 Zhang A, Zhang H, Zhou X, *et al.* Solitary fibrous tumors of the pleura shown on ^{18}F-FDG and ^{68}Ga-DOTA-FAPI-04 PET/CT. *Clin Nucl Med* 2021; 46: e534–e537.

110 Lapa C, Kircher S, Schirbel A, *et al.* Targeting CXCR4 with [^{68}Ga]Pentixafor: a suitable theranostic approach in pleural mesothelioma? *Oncotarget* 2017; 8: 96732–96737.

111 Graham MM, Gu X, Ginader T, *et al.* ^{68}Ga-DOTATOC imaging of neuroendocrine tumors: a systematic review and metaanalysis. *J Nucl Med* 2017; 58: 1452–1458.

112 Sharma P, Mukherjee A, Bal C, *et al.* Somatostatin receptor-based PET/CT of intracranial tumors: a potential area of application for ^{68}Ga-DOTA peptides? *AJR Am J Roentgenol* 2013; 201: 1340–1347.

113 Lococo F, Rapicetta C, Filice A, *et al.* The role of ^{68}Ga-DOTATOC PET/CT in the detection of relapsed malignant solitary fibrous tumor of the pleura. *Rev Esp Med Nucl Imagen Mol (Engl Ed)* 2018; 37: 257–258.

114 Lococo F, Rufini V, Filice A, *et al.* ^{68}Ga-DOTATOC PET/CT in pleural solitary fibrous tumors. *Clin Nucl Med* 2021; 46: e336–e338.

115 Coolen J, De Keyzer F, Nafteux P, *et al.* Malignant pleural disease: diagnosis by using diffusion-weighted and dynamic contrast-enhanced MR imaging – initial experience. *Radiology* 2012; 263: 884–892.

116 Murphy DJ, Mak SM, Mallia A, *et al.* Loco-regional staging of malignant pleural mesothelioma by integrated ^{18}F-FDG PET/MRI. *Eur J Radiol* 2019; 115: 46–52.

Suggested answers

1. d.
2. a: false; b: true; c: true; d: false.
3. c.